International Journal of Thermophysics, Vol. 8, No. 4, 1987

Hydrogen Component Fugacities in Binary Mixtures with Ethane: Temperature Dependence

T. J. Bruno[1] **and J. A. Schroeder**[1]

Received October 21, 1986

The fugacity coefficients of hydrogen in binary mixtures with ethane were measured using a physical equilibrium technique. This technique involves the use of an experimental chamber which is divided into two regions by a semipermeable membrane through which hydrogen, but not ethane, can penetrate. Measurement of the gas pressures inside and outside of the membrane allows a direct measurement of the hydrogen component fugacity coefficient at a given temperature and binary-mixture mole fraction. In this paper, results are reported at 101, 116, 141, 151, 160, and 190°C. In each case the total pressure of the mixture was maintained at 3.41 MPa. The qualitative features of the measurements are discussed and comparisons are made with predictions obtained from the Redlich–Kwong, Peng–Robinson, and extended corresponding-states models.

KEY WORDS: ethane; fugacity; hydrogen; mixtures.

1. INTRODUCTION

The fugacity of individual components of a mixture can, in principle, be calculated from an applicable equation of state (if the *PVT* surface of the gas mixture is known in the region of interest) using, for example,

$$\ln f_i = \ln Px_i + \int_0^P (V_i/RT - 1/P)\, dP \tag{1}$$

where f_i is the fugacity of component i, x_i is its mole fraction, V_i is its partial molar volume, P is the total pressure of the mixture, T is the temperature, and R is the gas constant. The need for a great deal of accurate

---

[1] Thermophysics Division, National Bureau of Standards, Boulder, Colorado 80303, U.S.A.

0195-928X/87/0700-0437$05.00/0

PVT data for the mixture and the limitations inherent in the application of many of the common equations of state to mixtures make this approach time-consuming and difficult. In the special case of gaseous mixtures containing hydrogen as one component, the physical equilibrium method provides a vast experimental simplification [1]. The problem of measuring the properties of a mixture is reduced to that of measuring the properties of a pure gas. A detailed description of the technique and its applications can be found elsewhere [2–4], so only a brief description is provided here.

An experimental chamber (usually a pressure vessel) is divided into two regions by a membrane which is permeable only to hydrogen. The membrane most often takes the form of a palladium–silver alloy (75% Pd, 25% Ag, by weight) fabricated into the form of a long section of thin-walled tubing. If one side of the membrane is charged with a gaseous mixture (of which hydrogen is a component) and the other side is initially evacuated, an equilibrium will eventually be established between the two sides of the membrane, with hydrogen gradually entering the evacuated space. The gradual approach to equilibrium is driven by the need to equalize the chemical potential of hydrogen on either side of the membrane. When equilibrium is actually reached in the system, the fugacity of hydrogen on both sides of the membrane must be equal [5–8].

Using appropriate instrumentation (which is described more fully in Section 2) the hydrogen partial pressure, P_{H_2}, and the mixture total pressure (outside the membrane), P_m, may be measured at a given temperature T and hydrogen mole fraction x_{H_2}. From these measurements, the fugacity of hydrogen can be computed. We can begin the process (at moderate pressures) using the pressure expansion of the virial equation of state (truncated after the third virial coefficient)

$$\ln \hat{\phi}_{H_2} = \left(\frac{P_{H_2}}{T}\right) + \left(\frac{C - B^2}{2R^2}\right)\left(\frac{P_{H_2}^2}{T^2}\right) \tag{2}$$

where B and C are the second and third virial coefficients, respectively, and $\hat{\phi}_{H_2}$ is the fugacity coefficient of pure hydrogen (which has permeated inside the membrane). The fugacity of (pure) hydrogen, $\hat{f}_{H_2}$, follows from

$$\hat{f}_{H_2} = \hat{\phi}_{H_2} P_{H_2} \tag{3}$$

Since pressure measurements are made when the system has reached equilibrium (that is, no net change in pressure or temperature with time on either side of the membrane), the fugacity of hydrogen must be the same on both sides of the membrane. Thus, the fugacity coefficient of hydrogen in the mixture is

$$f_{H_2} = \hat{f}_{H_2} = x_{H_2} P_{mm} \phi_{H_2}^{m} \tag{4}$$

where f_{H_2} and $\phi^m_{H_2}$ are the fugacity and fugacity coefficient, respectively, of hydrogen in the mixture.

2. EXPERIMENTAL

The apparatus used in this work is essentially the same as that used in previous studies [3–5] except for slight modifications in the configuration of the membrane manifold. In the current apparatus, the palladium/silver tubing (three sections, 396 cm long, 0.025 cm in wall thickness) which comprises the membrane has been formed into a larger network which penetrates more of the internal volume of the pressure vessel. This modification allows for somewhat faster equilibration times while eliminating the need for the magnetic linkage stirrer which was required previously.

The pressures of the pure hydrogen, P_{H_2}, and of the mixture, P_m, were measured using a commercial precision Bourdon tube pressure transducer, as valved through the manifold system described elsewhere [2]. This pressure transducer was calibrated through the range of interest using an air deadweight pressure balance (a secondary standard traceable to the NBS primary standard). The Bourdon tube transducer thus calibrated is accurate to within 0.04% over the range of the measurements. Temperature measurements were made using a commercial quartz crystal oscillator sensor. This thermometer is accurate to within 0.009°C over the range of these measurements and shows negligible hysteresis effects in the present situation of isothermal operation. In addition to this main thermometer, opposed pairs of type J thermocouples are used to sense temperature gradients between key components of the apparatus. These gradients are then minimized using very low-power shimming heaters (under manual control) located on or near the major components.

The mole fractions of the mixtures studied were determined using a developmental gas chromatograph and sampling system [9, 10]. The thermal conductivity detector was calibrated using the external standard method [9] with five standard mixtures of hydrogen + ethane which were prepared gravimetrically. Nitrogen was chosen as the carrier gas to provide a high sensitivity to hydrogen [11]. The chromatographic separations (for both the calibration and the actual fugacity measurements) were done using a packed column (2 m in length, 0.32 cm in o.d.) of Porapak-QS[2] of

---

[2] Certain commercial equipment, instruments, or materials are identified in this paper in order to specify adequately the experimental procedure. Such identification does not imply recommendation or endorsement by the National Bureau of Standards, nor does it imply that the materials or equipment identified are necessarily the best available for the purpose.

150 to 200 mesh. The column was maintained isothermally at 45.00 ± 0.02°C, with a carrier gas flow rate (volume, measured at the column exit) of 35 $\text{ml} \cdot \text{min}^{-1}$. The separation under these conditions is very favorable to precise quantitation. Baseline resolved peaks of reasonable width, convenient retention times, and excellent symmetry are easily obtained. The accuracy of the mole fractions thus obtained is approximately 0.5% for an equimolar mixture of hydrogen + ethane. Somewhat lower precision and accuracy are obtained at lower hydrogen mole fractions.

The hydrogen and ethane used in this work were research grade (99.995% purity for hydrogen, 99.99% purity for ethane), and no impurities were detected down to 1 ppm using subambient-temperature gas chromatography [12].

3. RESULTS AND DISCUSSION

Component fugacity coefficients of hydrogen in ethane, $\phi^{m}_{H_2}$, at nominal temperatures of 101, 116, 141, 151, 160, and 190°C are presented in Table I. The total pressure of the mixture was, on average, 3.41 ± 0.03 MPa. The actual measured values of the temperature and pressure for each isotherm are provided in the subheadings in Table I.

Table I. Measured Values of Hydrogen Component Fugacity Coefficients, $\phi^{m}_{H_2}$, at Mole Fractions x_{H_2}

x_{H_2}	$\phi^{m}_{H_2}$
$T = 100.98 \pm 0.03$°C $P = 3.40 \pm 0.05$ MPa	
0.262	1.087
0.581	1.043
0.713	1.032
0.799	1.025
0.876	1.020
$T = 116.02 \pm 0.03$°C $P = 3.43 \pm 0.04$ MPa	
0.511	1.053
0.667	1.038
0.776	1.029

Table I. *(Continued)*

x_{H_2}	$\phi^{m}_{H_2}$
$T = 140.00 \pm 0.03$°C $P = 3.43 \pm 0.02$ MPa	
0.595	1.043
0.735	1.032
0.772	1.029
0.878	1.022
$T = 150.99 \pm 0.02$°C $P = 3.45 \pm 0.05$ MPa	
0.433	1.062
0.561	1.048
0.612	1.037
0.835	1.024
0.887	1.021
0.952	1.016
$T = 160.00 \pm 0.03$°C $P = 3.37 \pm 0.04$ MPa	
0.216	1.070
0.428	1.052
0.557	1.043
0.676	1.035
0.767	1.029
0.811	1.026
0.891	1.021
0.935	1.019
$T = 190.00 \pm 0.02$°C $P = 3.39 \pm 0.01$ MPa	
0.345	1.061
0.519	1.044
0.651	1.034
0.757	1.027
0.824	1.022
0.858	1.020
0.901	1.017
0.925	1.015
0.949	1.014
0.964	1.013

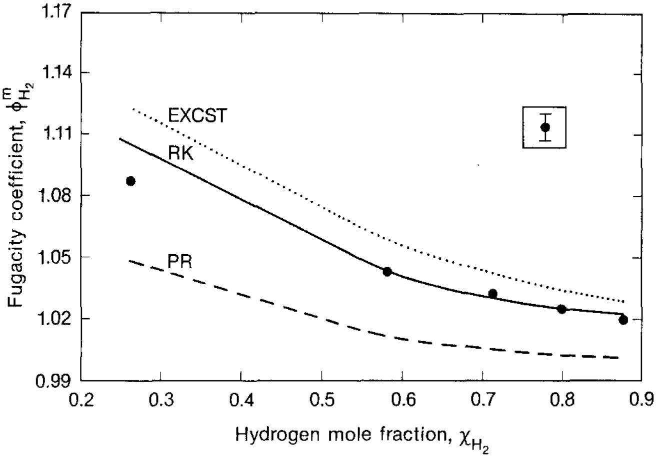

Fig. 1. A plot of fugacity coefficient, $\phi^m_{H_2}$, versus hydrogen mole fraction, x_{H_2}, at 101°C (374.15 K). The error bar in the box is typical for an equimolar mixture.

Plots of $\phi^m_{H_2}$ versus hydrogen mole fraction are provided in Figs. 1 through 6. The experimental points in these figures are represented as filled circles. The error bars (enclosed in the boxes in the figures) represent the uncertainty of a $\phi^m_{H_2}-x_{H_2}$ pair for an equimolar mixture (an error of approximately 1.1%). A detailed error analysis describing how the magnitude of the uncertainty was arrived at has been presented previously [2].

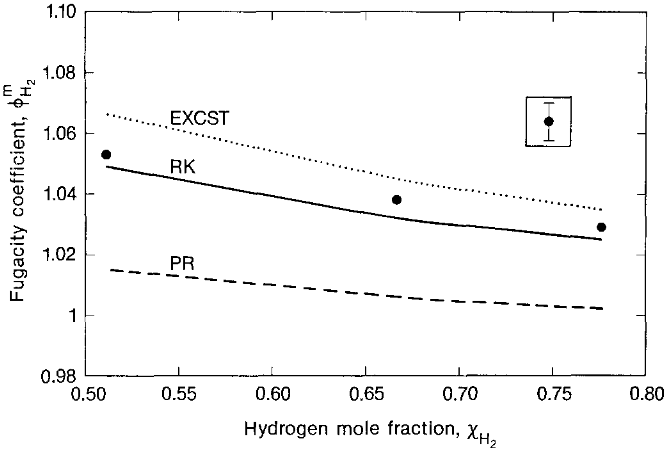

Fig. 2. A plot of fugacity coefficient, $\phi^m_{H_2}$, versus hydrogen mole fraction, x_{H_2}, at 116°C (389.15 K). The error bar in the box is typical for an equimolar mixture.

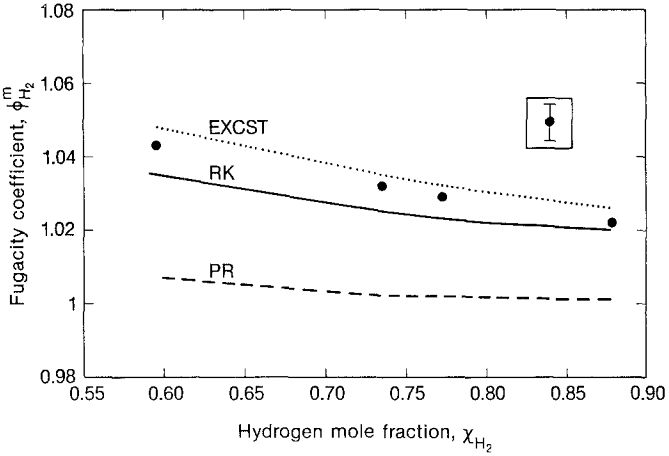

Fig. 3. A plot of fugacity coefficient, $\phi_{H_2}^m$, versus hydrogen mole fraction, x_{H_2}, at 141°C (414.15 K). The error bar in the box is typical for an equimolar mixture.

Before examining the agreement of the experimental data with predictions using selected equations of state, some qualitative observations may be made. The change of $\phi_{H_2}^m$ with hydrogen mole fraction is more pronounced at lower values of x_{H_2}, leveling off at the higher values. This observation is consistent for a gas of a low molecular weight in a micture with gas of a higher molecular weight. It should be noted, however, that this

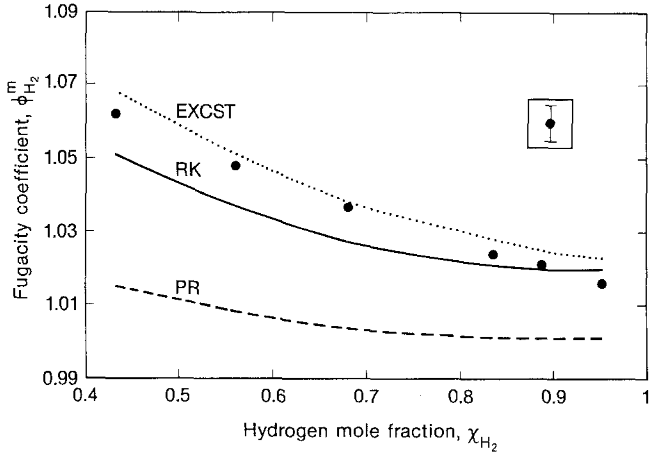

Fig. 4. A plot of fugacity coefficient, $\phi_{H_2}^m$, versus hydrogen mole fraction, x_{H_2}, at 151°C (424.15 K). The error bar in the box is typical for an equimolar mixture.

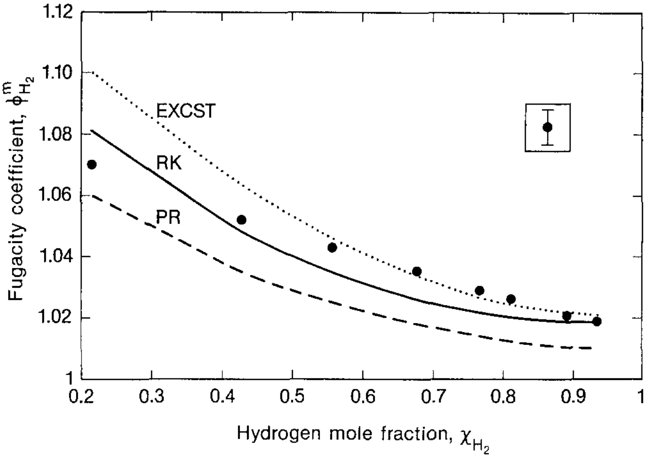

Fig. 5. A plot of fugacity coefficient, $\phi_{H_2}^m$, versus hydrogen mole fraction, x_{H_2}, at 160°C (433.15 K). The error bar in the box is typical for an equimolar mixture.

change in plot curvature is much less pronounced with the hydrogen + ethane binary than was noted in binary mixtures of hydrogen with propane and carbon dioxide [3–5]. The total change in $\phi_{H_2}^m$ over the mole fraction range is also lower for the hydrogen + ethane binary. These observations are indicative of somewhat less nonideality in the ethane binary than in the propane or carbon dioxide binaries.

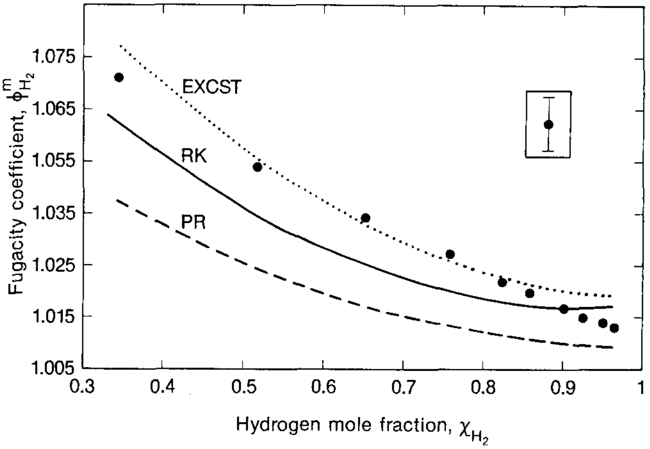

Fig. 6. A plot of fugacity coefficient, $\phi_{H_2}^m$, versus hydrogen mole fraction, x_{H_2}, at 190°C (463.15 K). The error bar in the box is typical for an equimolar mixture.

It will be noted upon examination of the data in Table I that the effect of temperature on the fugacity coefficient is relatively small, at least for the temperature range considered in this work. The effect of temperature is most pronounced in the region of low hydrogen mole fractions, while in the high-mole fraction range it appears lost in the "noise" of experimental error. This provides an excellent opportunity to test equations of state for their ability to predict this relatively small temperature dependence.

At the pressures encountered in this work, equations of state provide the simplest avenue to obtaining predictions of fugacity coefficients of gaseous mixtures. The common approaches involve either cubic equations of state or the extended corresponding-state approach (EXCST). In this study we have applied both methods. As an example of a cubic equation of state, we have used the popular Peng–Robinson (PR) modification of the Redlich–Kwong (RK) equation [13]. For comparative purposes and as a matter of interest, we have also used the unmodified Redlich–Kwong equation of state, the simplest of the cubic equations [14] (with the exception of the Van der Waals equation). The extended corresponding-states model we have used employs propane (using a 32-term Benedict–Webb–Rubin equation) as the reference fluid [3, 15].

In Figs. 1 through 6, the solid line represents the predictions of the simple Redlich–Kwong equation of state. The dashed line was generated from the predictions of the Peng–Robinson equation, and the doted line from the extended corresponding-states approach. Van der Waals mixing rules have been used throughout. In the calculations from the Peng–Robinson and extended corresponding-states models, the acentric factor for hydrogen ω was assigned a value of -0.22. This is the experimentally measured value as obtained from vapor pressure measurements [8]. It should be noted that the predictions are not very sensitive to changes in the acentric factor. The calculated values are usually within 1% as long as physically reasonable values (-0.22 or 0) are used. Binary interaction coefficients were assigned a value of zero.

While all of the models considered appear to give reasonable predictions (within 2–3% of the measured values), the best predictions overall are provided by the extended corresponding-states approach. Despite the inherent simplicity of the Redlich–Kwong equation of state, it also gives very good predictions. In some cases (the entire mole fraction range at 101°C, for example), the predictions from the Redlich–Kwong equation are better than those obtained from the more sophisticated extended corresponding-states approach. The Peng–Robinson equation of state, on the other hand, consistently predicts fugacity coefficients which are too low.

At each temperature, the largest derivations of the experimental data from the predictions are to be found in the low-hydrogen mole fraction region. This characteristic has been observed in all measurements of this type and is caused by the lower chromatographic precision obtainable at the low end of the mole fraction range.

As was stated earlier, the effect of temperature on the ϕ_{H_2} values is very small, especially in the high-hydrogen mole fraction range. A single plot containing all of the isotherms does show a somewhat larger effect due to temperature in the low-hydrogen mole fraction region. Such a plot is not included in this paper since there are relatively few measured data points in this area. In addition, the points between x_{H_2} values of 0.6 and 1 converge into a confusing jumble, with any structure lost in the experimental error. All of the equations of state predict a low dependence on temperature, especially in the high-x_{H_2} range. For example, the extended corresponding-states model predicts a decrease in the fugacity coefficient (at an x_{H_2} value of 0.6) of 2.2% upon raising the system temperature from 353 to 463 K. This change in the fugacity coefficient drops to 0.5% at a hydrogen mole fraction of 1. For this same temperature increment, the Redlich–Kwong equation also predicts a change of 0.5% at $x_{H_2} = 1$, while the Peng–Robinson equation predicts a smaller change. This behavior with temperature is displayed qualitatively by the data measured in this study. A study of the effect of pressure on the fugacity coefficient is currently in progress and will be reported on later.

4. CONCLUSIONS

Component fugacity coefficients for the hydrogen + ethane binary system were measured along six isotherms, at a total-mixture pressure of 3.41 MPa, using the physical equilibrium technique. The experimental data were used to evaluate the predictive ability of three equation-of-state approaches. The prediction were found to be good in general, with the extnded corresponding-states approach and the Redlich–Kwong equation of state providing better values than the Peng–Robinson equation of state. The observed temperature dependence, while slight, is also qualitatively predicted.

ACKNOWLEDGMENTS

The authors would like to thank James F. Ely of the National Bureau of Standards Thermophysics Division for several valuable discussions. The financial support of the Gas Research Institute is gratefully acknowledged.

REFERENCES

1. H. Y. Cheh, *Proc. 6th Symp. Thermophys. Prop.* (ASME, New York, 1973), p. 256.
2. T. J. Bruno, *J. Res. Natl. Bur. Stand. (U.S.)* **90**(2):127 (1985).
3. T. J. Bruno, G. L. Hume, and J. F. Ely, *Int. J. Thermophys.* **7**:1033 (1986).
4. T. J. Bruno and G. L. Hume, *Int. J. Thermophys.* **7**:1053 (1986).
5. T. J. Bruno, *Int. J. Thermophys.* **8**:205 (1987).
6. S. I. Sandler, *Chemical and Engineering Thermodynamics* (John Wiley and Sons, New York, 1977).
7. B. G. Kyle, *Chemical and Process Thermodynamics* (Prentice Hall, Englewood Cliffs, N.J., 1984).
8. J. M. Prausnitz, *Molecular Thermodynamics of Fluids Phase Equilibria* (Prentice Hall, Englewood Cliffs, N.J., 1964).
9. T. J. Bruno, *J. Chromatogr. Sci.* **23**:325 (1985).
10. T. J. Bruno and J. G. Shepherd, *Anal. Chem.* **58**:671 (1986).
11. T. J. Bruno and P. D. N. Svoronos, *Basic Tables for Chemical Analysis*, Natl. Bur. Stand. (U.S.), Technical Note 1096 (1986).
12. T. J. Bruno, *Anal. Chem.* **58**:1596 (1986).
13. D.-Y. Peng and D. B. Robinson, *Ind. Eng. Chem. Fund.* **15**:59 (1976).
14. J. M. Smith and H. C. Van Ness, *Introduction to Chemical Engineering Thermodynamics* (McGraw–Hill, New York, 1975).
15. J. F. Ely, *Proc. 63rd. Gas Process. Assoc. Conv.* **9** (1984).